AD A138 279 SMALL STEEL PROJECTILE FIRINGS AGAINST SIMULATED REINFORCED CONCRETE SLAB..(U) NAVAL WEAPONS CENTER CHINA LAKE CA J C SCHULZ ET AL. JAN 84 NWC-TP-6501 1/1

UNCLASSIFIED SBI-AD-E900 320 F/G 19/1 NL

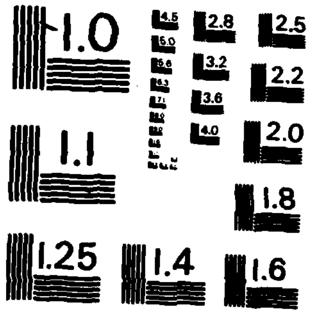

MICROCOPY RESOLUTION TEST CHART
NATIONAL BUREAU OF STANDARDS-1963-A

UNCLASSIFIED

SECURITY CLASSIFICATION OF THIS PAGE (When Data Entered)

REPORT DOCUMENTATION PAGE

READ INSTRUCTIONS BEFORE COMPLETING FORM

1. REPORT NUMBER NWC TP 6501	2. GOVT ACCESSION NO. AD-A138 279	3. RECIPIENT'S CATALOG NUMBER
4. TITLE (and Subtitle) SMALL STEEL PROJECTILE FIRINGS AGAINST SIMULATED REINFORCED CONCRETE SLABS AT NORMAL INCIDENCE AND OBLIQUITY		5. TYPE OF REPORT & PERIOD COVERED Research Report FY 1982–1983
		6. PERFORMING ORG. REPORT NUMBER
7. AUTHOR(s) J. C. Schulz O. E. R. Heimdahl S. Finnegan		8. CONTRACT OR GRANT NUMBER(s)
9. PERFORMING ORGANIZATION NAME AND ADDRESS Naval Weapons Center China Lake, California 93555		10. PROGRAM ELEMENT, PROJECT, TASK AREA & WORK UNIT NUMBERS AIRTASK A32-321C/008B/3F32-300-000 Appropriation 1731319.41AJ
11. CONTROLLING OFFICE NAME AND ADDRESS Naval Weapons Center China Lake, California 93555		12. REPORT DATE January 1984
		13. NUMBER OF PAGES 54
14. MONITORING AGENCY NAME & ADDRESS(if different from Controlling Office)		15. SECURITY CLASS. (of this report) UNCLASSIFIED
		15a. DECLASSIFICATION/DOWNGRADING SCHEDULE

16. DISTRIBUTION STATEMENT (of this Report)

Approved for public release; distribution unlimited.

17. DISTRIBUTION STATEMENT (of the abstract entered in Block 20, if different from Report)

18. SUPPLEMENTARY NOTES

19. KEY WORDS (Continue on reverse side if necessary and identify by block number)

Impact Survivability
Projectile Impact

20. ABSTRACT (Continue on reverse side if necessary and identify by block number)

See back of form.

DD FORM 1 JAN 73 1473 EDITION OF 1 NOV 65 IS OBSOLETE
S/N 0102-LF-014-6601

UNCLASSIFIED

SECURITY CLASSIFICATION OF THIS PAGE (When Data Entered)

UNCLASSIFIED

SECURITY CLASSIFICATION OF THIS PAGE (When Data Entered)

(U) *Small Steel Projectile Firings Against Simulated Reinforced Concrete Slabs at Normal Incidence and Obliquity*, by J. C. Schulz, O. E. R. Heimdahl, and S. Finnegan. China Lake, Calif., Naval Weapons Center, January 1984. 54 pp. (NWC TP 6501, publication UNCLASSIFIED.)

(U) Experimental firings of small blunt-nosed cylindrical steel projectiles against simulated reinforced concrete slabs at normal incidence and obliquity were conducted. Both unfilled projectiles and projectiles filled with an explosive simulant (plasticine) were fired. Slab thicknesses ranged from one to ten projectile diameters. The deformed shapes and exit velocities of the projectiles were determined. These data will be used for the verification of a new technique being developed for finite element modeling of blunt projectile response to target impact.

UNCLASSIFIED

SECURITY CLASSIFICATION OF THIS PAGE(When Data Entered)

CONTENTS

Introduction	3
Description of Experiments	3
Projectiles	3
Slab Targets	4
Test Procedure	5
Normal Incidence Results	5
Oblique Incidence Results	14
Plug Formation	14
Conclusions	21
Appendix A. Photographs of Projectiles Fired at Normal Incidence	23
Appendix B. Photographs of Projectiles Fired at 45 Degrees Obliquity	41

INTRODUCTION

Several sets of experimental firings of small, blunt-nosed cylindrical steel projectiles against semi-infinite simulated concrete and thin steel plate targets at normal incidence and obliquity have been previously reported.[1-4] This report describes firings of similar projectiles against simulated reinforced concrete slabs. Slab thicknesses ranged from one to ten projectile diameters. Both unfilled projectiles and projectiles filled with an explosive simulant (plasticine) were used. Firings were made at three nominal impact velocities (1,800, 2,100, and 2,400 ft/s) selected to produce slight, moderate, and severe bulging of the projectiles, respectively. Impacts were at normal incidence and 45 degrees obliquity.

The purpose of these firings was to collect data regarding the deformed shapes (increase in radius at nose, increase in radius at cavity bulge, and decrease in length) and the exit velocities (penetration depths where perforation did not occur) of the projectiles that can be used for verification of a new technique for the finite element modeling of the structural response of blunt projectiles to impact against slab targets. A report describing this new technique (the target plug approach) is being written.

DESCRIPTION OF EXPERIMENTS

PROJECTILES

The test projectiles were flat-fronted, hollow steel cylinders, 2 inches long and 0.5 inch in diameter, having an internal cavity with a hemispherical front end. The front of the cavity was 0.25 inch from the front of the projectile and the cavity wall was 0.04 inch thick. The

----

[1] W. J. Stronge and J. C. Schulz. "Projectile Impact Damage Analysis," in *Papers Presented at the Symposium on Computational Methods in Non-linear Structural and Solid Mechanics*, Arlington, Virginia, 6-8 October 1980, ed. by Ahmed K. Noor and Harvey G. McComb, Jr. New York, Pergamon Press, 1981. (Also published as special issue of *J. Computers and Structures*, Vol. 13, No. 1-2 (1981), pp. 287-294.)

[2] Naval Weapons Center. *Survivability of Penetrators With Circumferential Shear-Control Grooves*, by J. C. Schulz and O. E. R. Heimdahl. China Lake, Calif., NWC, April 1981. (NWC TP 6275, publication UNCLASSIFIED.)

[3] Naval Weapons Center. *Oblique Impact Projectile Damage*, by J. C. Schulz and O. E. R. Heimdahl. China Lake, Calif., NWC, January 1982. (NWC TM 4695, publication UNCLASSIFIED.)

[4] Naval Weapons Center. *Effects of Longitudinal Grooves on Survivability of Cylindrical Steel Projectiles Fired Against Simulated Concrete Targets*, by O. E. R. Heimdahl and J. C. Schulz. China Lake, Calif., NWC, November 1982. (NWC TP 6402, publication UNCLASSIFIED.

projectiles were machined from 4340 steel rods and were heat-treated to a Rockwell "C" hardness of 38-40. Half of the projectiles were filled with plasticine (a wax-based modeling material) and half were left unfilled. A cross-sectional view of a filled projectile is shown in Figure 1. The unfilled projectiles were similar except for the absence of the filler. The projectiles were plated with a thin layer (about 0.0005 inch) of copper to reduce abrasion of the gun barrel.

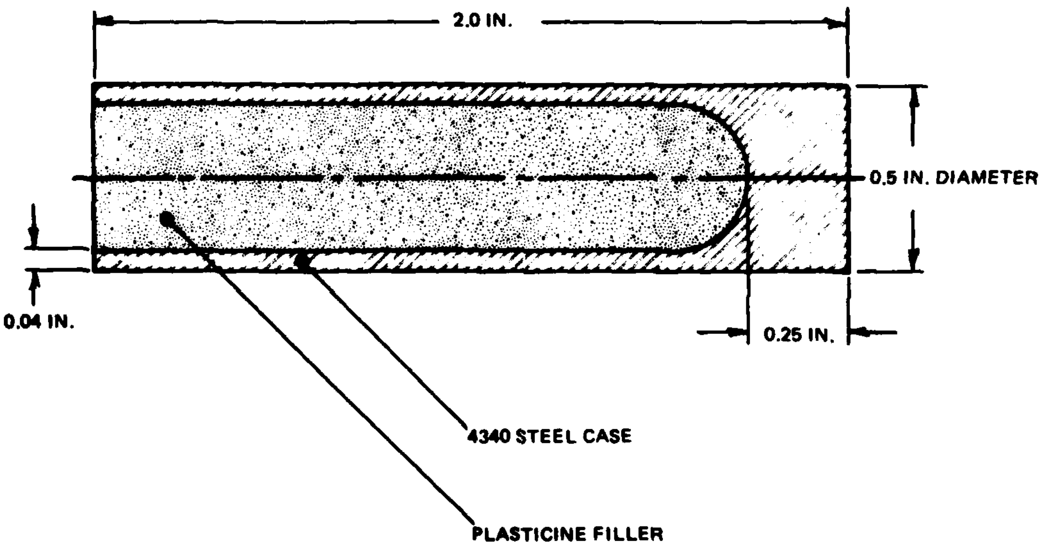

FIGURE 1. Cross-Sectional View of Filled Projectile.

SLAB TARGETS

The simulated reinforced concrete slab targets were made of Thorite (registered trademark of Standard Drywall Products), a fast-setting, high-strength (3,950 psi compressive strength) concrete patching compound consisting of sand, cement, and additives to promote rapid curing. The largest sand grains were about 0.04 inch in diameter. Slabs were fabricated in four thicknesses (0.5, 1, 2.5, and 5 inches) and were 10 by 10 inches square, transverse to the thickness. Layers of half-inch wire mesh (hardware cloth) spaced 0.5 inch apart over the thickness were used for the reinforcement. The soft steel wire used in the mesh was 0.05 inch in diameter (18 gauge). There were 1, 2, 5, and 10 layers of mesh in the 0.5-, 1-, 2.5-, and 5-inch-thick slabs, respectively. The targets were cured 7 days prior to firing.

TEST PROCEDURE

The projectiles were fired from a smooth-bore 50-caliber powder gun. Target impact velocities were measured in the gun barrel with a photo diode system coupled to an interval counter. The targets were placed about 6 inches from the end of the barrel. Exit velocities from the target were determined from Kerr Cell photographs. Projectiles were captured in a recovery trough filled with Celotex slabs placed immediately behind the targets. The apparatus is described more fully by Goldsmith and Finnegan.[5]

NORMAL INCIDENCE RESULTS

Forty-eight normal incidence firings were made. Results for unfilled and filled projectiles are summarized in Tables 1 and 2, respectively. Photographs of the projectiles after normal incidence impact are shown in Appendix A. Projectile deformation is characterized by slight mushrooming at the nose, development of a bulge near the front of the internal cavity, and overall shortening of the projectile length.

Plots of exit velocity versus impact velocity for unfilled and filled projectiles are shown in Figures 2 and 3, respectively. Exit velocities are higher for filled projectiles, as would be expected from their greater mass.

Plots of radius increase at the nose versus impact velocity for unfilled and filled projectiles are shown in Figures 4 and 5. The radius increase at the nose appears independent of slab thickness and presence or absence of filler. The single line drawn through the points is the same in both figures. The implication is that the radius increase at the nose is due to the high transient stresses associated with initial impact with the slab surface and occurs extremely quickly. By the time differences in slab thickness or projectile filling can affect the nose through propagation of stress waves, the radius increase is already complete.

Plots of radius increase at the cavity bulge versus impact velocity for unfilled and filled projectiles are shown in Figures 6 and 7. Within the scatter of the data, the radius increases at the cavity bulge for projectiles impacting 1-, 2.5-, and 5-inch-thick slabs are the same (and indicated by a single dashed line). Bulging of projectiles impacting 0.5-inch-thick slabs is considerably less. This indicates that most bulging in the cavity region occurs before the projectile has penetrated two diameters into the slab.

Plots of decrease in length versus impact velocity are shown in Figures 8 and 9. Again, the results from projectiles impacting 1-, 2.5-, and 5-inch-thick slabs are the same. This is not surprising because much of the decrease in length is a consequence of formation of the bulge.

----

[5] W. Goldsmith and S. A. Finnegan. "Penetration and Perforation Processes in Metal Targets At and Above Ballistic Velocities," *Intl. J. Mech. Sci.*, Vol. 13 (1971), pp. 843-866.

TABLE 1. Unfilled Projectile Normal Incidence Slab Firing Results.

Slab thickness, in.	Projectile mass, g	Impact velocity, ft/s	Exit velocity, ft/s	Nose diameter, in.	Cavity bulge diameter, in.	Length, in.
0.5	19.94	1,795	1,502	0.504	0.515	1.990
0.5	20.14	1,800	1,448	0.507	0.513	1.989
0.5	19.87	2,110	1,645	0.514	0.522	1.975
0.5	20.17	2,135	1,784	0.509	0.526	1.974
0.5	19.97	2,370	1,935	0.520	0.532	1.960
0.5	20.03	2,400	1,901	0.519	0.553	1.950
1.0	20.06	1,785	1,400	0.509	0.515	1.988
1.0	20.06	1,840	1,339	0.508	0.519	1.984
1.0	19.94	2,110	1,516	0.508	0.536	1.964
1.0	19.95	2,160	1,621	0.516	0.537	1.963
1.0	20.11	2,340	1,739	0.515	0.563	1.938
1.0	19.97	2,405	1,820	0.528	0.580	1.924
2.5	20.29	1,765	728	0.503	0.515	1.989
2.5	20.24	1,800	761	0.506	0.521	1.982
2.5	19.96	2,055	960	0.509	0.536	1.976
2.5	19.82	2,110	962	0.508	0.539	1.964
2.5	20.09	2,365	1,223	0.521	0.566	1.936
2.5	20.05	2,420	a	0.529	a	a
5.0	19.87	1,805	3.2[b]	0.504	0.520	1.988
5.0	20.20	1,810	2.8[b]	0.502	0.521	1.982
5.0	19.92	2,130	2.6[b]	0.507	0.534	1.963
5.0	19.73	2,160	238	0.508	0.534	1.969
5.0	19.96	2,410	c	0.528	0.563	1.935
5.0	20.01	2,425	0	0.518	0.588	1.913

[a] Quantity could not be measured, projectile broke up.
[b] Projectile did not perforate, quantity given is penetration depth, in.
[c] Exit velocity could not be determined from Kerr Cell camera data.

TABLE 2. Filled Projectile Normal Incidence Slab Firing Results.

Slab thickness, in.	Projectile mass, g	Impact velocity, ft/s	Exit velocity, ft/s	Nose diameter, in.	Cavity bulge diameter, in.	Length, in.
0.5	26.34	1,770	1,608	0.507	0.521	1.987
0.5	26.51	1,785	1,595	0.504	0.520	1.986
0.5	26.36	2,070	1,783	0.517	0.530	1.974
0.5	26.45	2,135	1,789	0.515	0.534	1.971
0.5	26.47	2,380	2,118	0.518	0.548	1.958
0.5	26.34	2,385	2,147	0.518	0.550	1.958
1.0	26.39	1,825	1,455	0.502	0.518	1.987
1.0	26.42	1,840	1,434	0.503	0.520	1.989
1.0	26.18	2,070	1,574	0.513	0.535	1.967
1.0	26.41	2,105	1,674	0.514	0.540	1.964
1.0	26.33	2,370	1,921	0.518	0.588	1.932
1.0	26.42	2,380	2,001	0.519	0.590	1.931
2.5	26.47	1,755	1,075	0.503	0.522	1.984
2.5	26.13	1,805	1,026	0.509	0.520	1.984
2.5	26.39	2,110	1,223	0.510	0.540	1.963
2.5	26.42	2,120	1,261	0.515	0.557	1.956
2.5	26.49	2,360	1,470	0.522	0.591	1.925
2.5	26.42	2,410	1,486	0.519	0.624	1.904
5.0	26.38	1,770	5.1[a]	0.502	0.523	1.983
5.0	26.41	1,775	126	0.503	0.525	1.982
5.0	26.40	2,045	435	0.509	0.554	1.959
5.0	26.43	2,130	688	0.512	0.554	1.955
5.0	26.17	2,380	800	0.520	0.593	1.923
5.0	26.51	2,400	762	0.524	0.620	1.904

[a] Projectile did not perforate, quantity given is penetration depth, in.

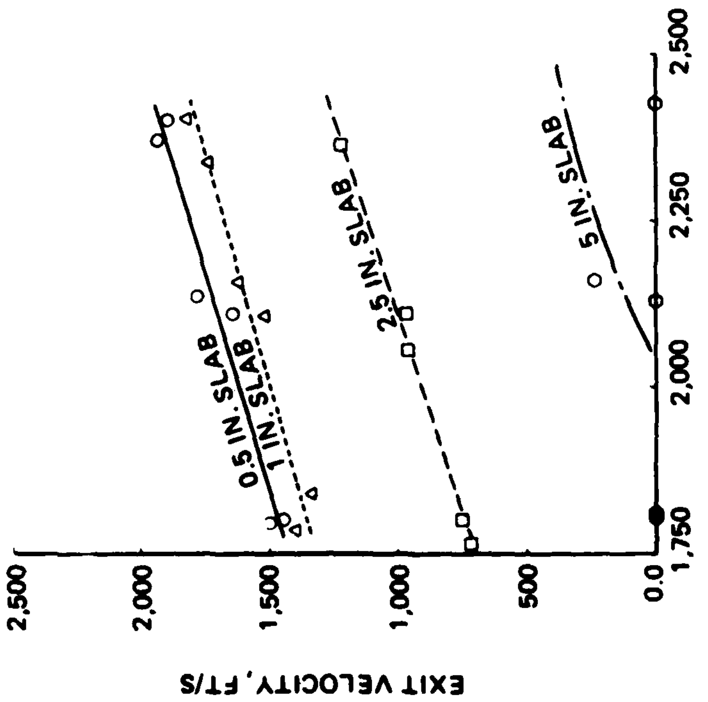

FIGURE 2. Exit Velocity vs. Impact Velocity for Unfilled Projectiles After Normal Incidence Slab Impact.

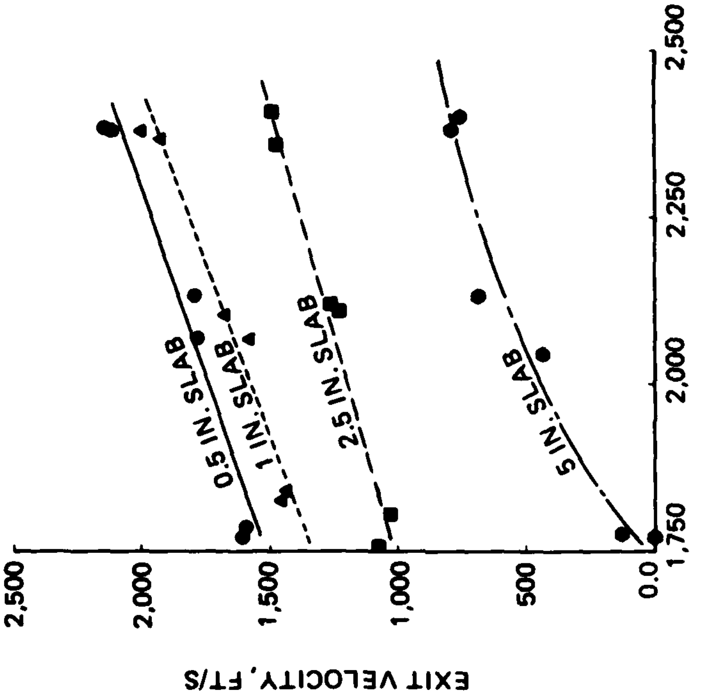

FIGURE 3. Exit Velocity vs. Impact Velocity for Filled Projectiles After Normal Incidence Slab Impact.

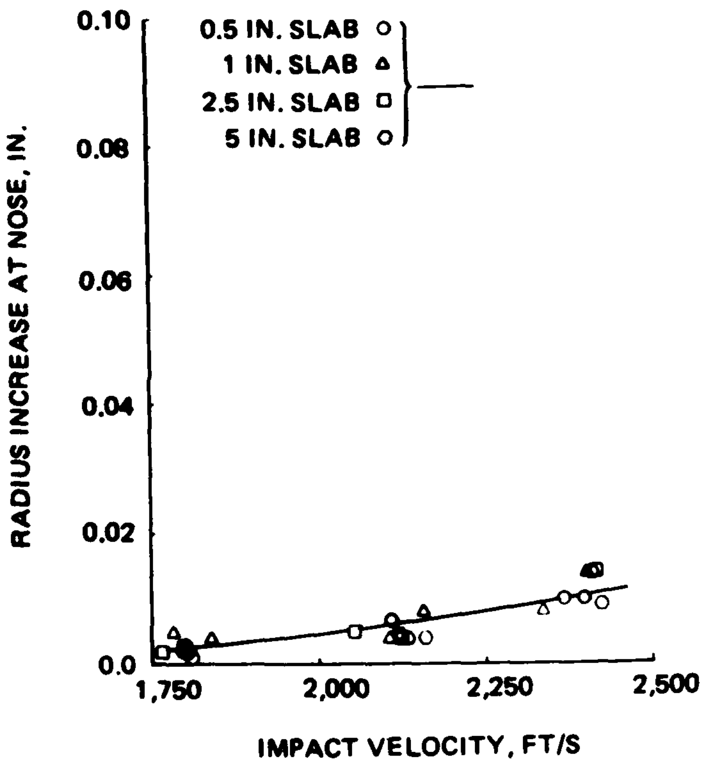

FIGURE 4. Radius Increase at Nose vs. Impact Velocity for Unfilled Projectiles After Normal Incidence Slab Impact.

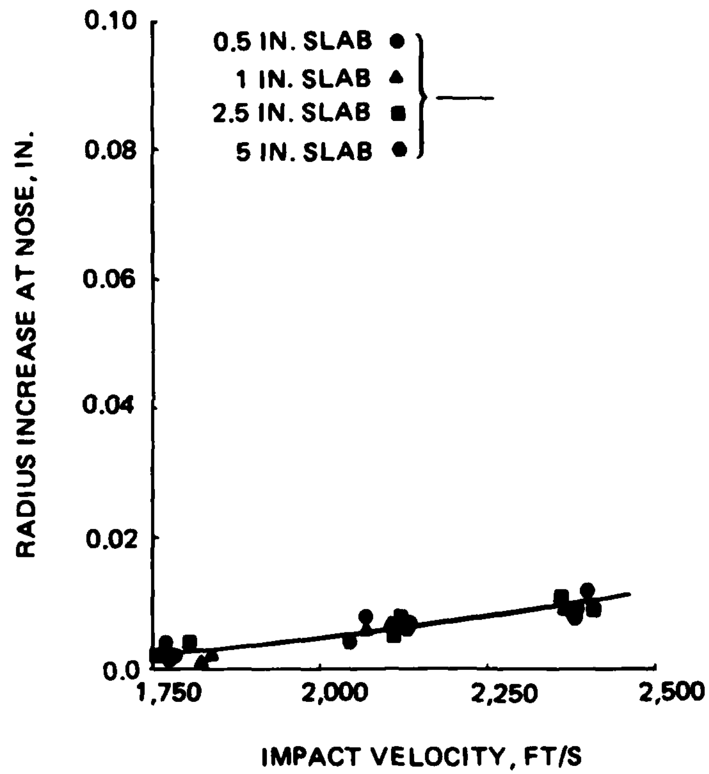

FIGURE 5. Radius Increase at Nose vs. Impact Velocity for Filled Projectiles After Normal Incidence Slab Impact.

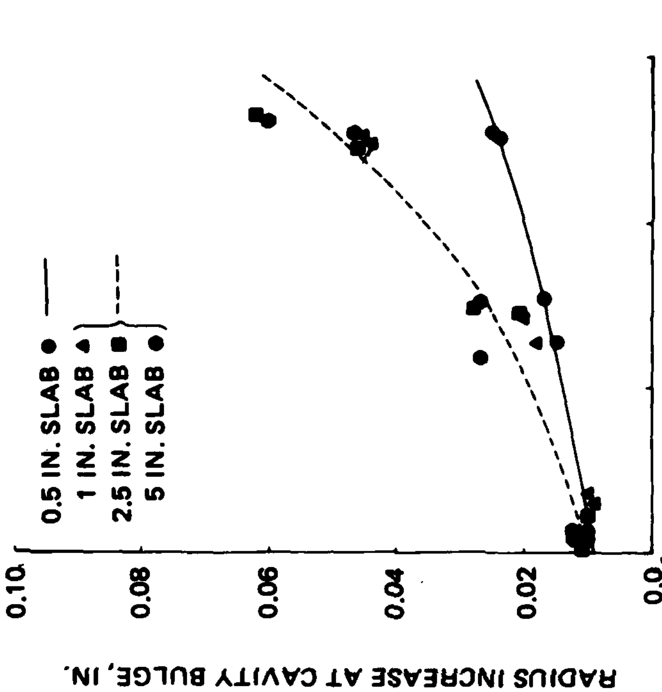

FIGURE 7. Radius Increase at Cavity Bulge vs. Impact Velocity for Filled Projectiles After Normal Incidence Slab Impact.

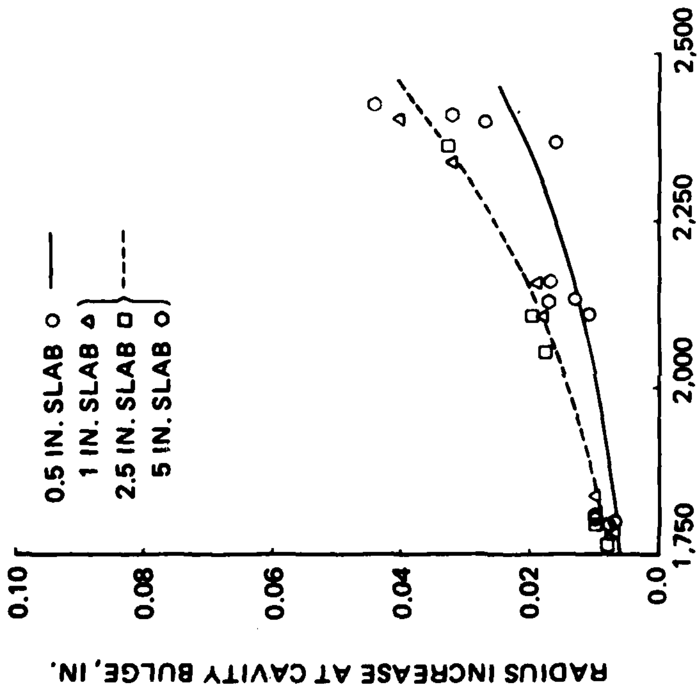

FIGURE 6. Radius Increase at Cavity Bulge vs. Impact Velocity for Unfilled Projectiles After Normal Incidence Slab Impact.

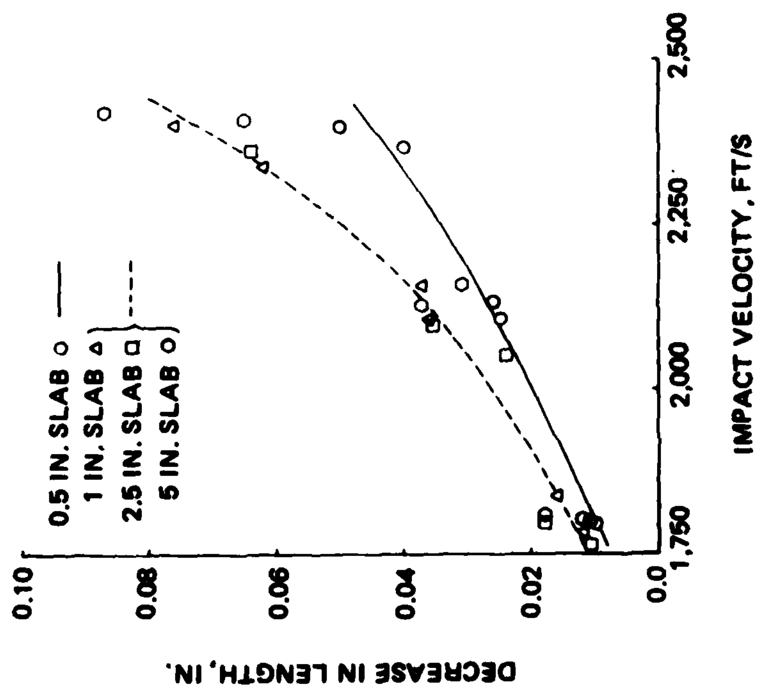

FIGURE 8. Decrease in Length vs. Impact Velocity for Unfilled Projectiles After Normal Incidence Slab Impact.

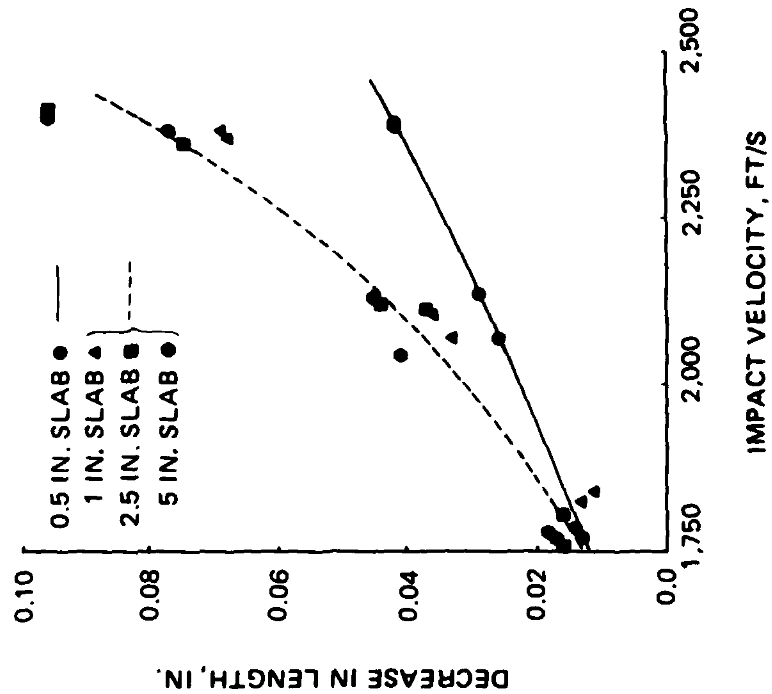

FIGURE 9. Decrease in Length vs. Impact Velocity for Filled Projectiles After Normal Incidence Slab Impact.

OBLIQUE INCIDENCE RESULTS

Thirty-six firings at 45 degrees obliquity were made against the 0.5-, 1-, and 2.5-inch-thick slabs only. Results for unfilled and filled projectiles are summarized in Tables 3 and 4, respectively. Photographs of the projectiles after oblique incidence impact are shown in Appendix B. In addition to mushrooming at the nose and developing a cavity bulge, the projectiles impacting at obliquity also bent such that the nose of the projectile was canted with respect to the cylindrical case.

Plots of exit velocity versus impact velocity for unfilled and filled projectiles are shown in Figures 10 and 11, respectively. Exit velocities were lower for the oblique incidence firings due to the greater distance traveled by the projectiles across the slab. The apparent decrease in exit velocity with increasing impact velocity for the filled projectiles against 2.5-inch-thick slabs may be due to the extreme bulging of these projectiles.

Plots of radius increase at the nose versus impact velocity for unfilled and filled projectiles are shown in Figures 12 and 13. Radius growth at the nose was less for the projectiles fired at obliquity where the entire front surface does not contact the surface of the slab simultaneously.

Plots of radius increase at the cavity bulge versus impact velocity for unfilled and filled projectiles are shown in Figures 14 and 15. Bulging in the cavity region was greater for projectiles fired at obliquity. Also, the effect of slab thickness appeared more significant.

Plots of bend angle versus impact velocity for unfilled and filled projectiles are shown in Figures 16 and 17. Bending is much greater for filled projectiles. The projectiles were not marked prior to firing so the direction of bending could not be determined. However, based on previous oblique incidence firing data,[3] it is probable that bending was such that the leading edge (side of front surface contacting target first) moved nearer the rear of the case.

PLUG FORMATION

It has been shown experimentally[6] that roughly conical plugs of target material form on the front of blunt steel projectiles impacting thick plaster of Paris and simulated concrete targets. These plugs form early in the penetration process and are carried along by the projectiles until they come to rest. Plugs form during penetration into plaster of Paris at both normal incidence and 45 degrees obliquity. Only normal incidence shots were made against simulated concrete so it is an open question as to whether plugs form at obliquity against this target material.

The presence or absence of a plug on the front of a blunt projectile is of interest with regard to the determination of the drag force exerted by the target material on the projectile. This force can be expected to be less (and its distribution different) if the front surface is

----

[6] M. E. Backman, S. A. Finnegan and K. G. Whitham. "The Formation of Stagnation Zones in Stable Penetrations of Brittle Materials," in *Proceedings of the Sixth International Symposium on Ballistics, Orlando, Fla., 27-29 October 1981.* Columbus, Ohio, Battelle Columbus Laboratories, 1981. (Publication UNCLASSIFIED.)

TABLE 3. Unfilled Projectile Oblique Incidence Slab Firing Results.

Slab thickness, in.	Projectile mass, g	Impact velocity, ft/s	Exit velocity, ft/s	Nose diameter, in.	Cavity bulge diameter, in.	Bend angle, deg.
0.5	19.20	1,807	1,414	0.502	0.510	1.0
0.5	19.63	1,842	1,361	0.503	0.517	1.5
0.5	19.49	2,150[a]	1,573	0.508	0.547	2.5
0.5	19.50	2,165	1,717	0.510	0.544	2.5
0.5	19.66	2,440	1,974	0.515	0.563	3.0
0.5	19.88	2,467[a]	1,934	0.510	0.565	3.0
1.0	19.77	1,756	1,013	0.508	0.511	2.0
1.0	19.68	1,800	1,052	0.503	0.513	2.0
1.0	19.71	2,125	1,330	0.506	0.560	4.5
1.0	19.60	2,140	1,336	0.509	0.551	3.5
1.0	19.42	2,440	1,622	0.510	*b*	*b*
1.0	19.35	2,495	1,558	0.509	*b*	*b*
2.5	19.68	1,766	0[c]	0.504	0.517	2.0
2.5	19.58	1,800	0[c]	0.501	0.519	3.0
2.5	19.67	2,145	0[c]	0.505	0.571	6.0
2.5	19.83	2,170	0[c]	0.506	0.565	5.5
2.5	19.95	2,310	*b*	0.504	*b*	*b*
2.5	19.54	2,370	*b*	0.507	*b*	*b*

[a] Estimated, impact velocity could not be determined.
[b] Quantity could not be measured, projectile broke up or damaged too badly.
[c] Projectile did not perforate.

TABLE 4. Filled Projectile Oblique Incidence Slab Firing Results.

Slab thickness, in.	Projectile mass, g	Impact velocity, ft/s	Exit velocity, ft/s	Nose diameter, in.	Cavity bulge diameter, in.	Bend angle, deg.
0.5	26.26	1,773	1,443	0.503	1.514	0.5
0.5	26.04	1,809	1,484	0.504	0.519	1.5
0.5	26.25	2,085	1,851	0.506	0.523	0.0
0.5	26.21	2,120	1,787	0.508	0.548	0.5
0.5	26.07	2,380	2,027	0.511	0.576	2.0
0.5	26.07	2,445	2,081	0.510	0.591	2.5
1.0	26.10	1,843	1,260	0.503	0.527	1.0
1.0	26.16	1,862	1,284	0.503	0.531	2.0
1.0	26.23	2,095	1,524	0.511	0.579	4.0
1.0	26.00	2,170	1,594	0.508	0.601	3.5
1.0	26.14	2,365	1,665	0.509	0.686[a]	11.0[a]
1.0	26.08	2,405	1,713	0.512	0.671[a]	6.0[a]
2.5	26.23	1,813	400	0.504	0.535	1.5
2.5	26.17	1,818	354	0.503	0.538	2.5
2.5	26.06	2,125	0[b]	0.504	0.670[a]	9.0[a]
2.5	26.09	2,130	0[b]	0.503	0.731[a]	11.5[a]
2.5	26.23	2,180	c	0.505	c	c
2.5	26.13	2,235	c	0.508	c	c

[a] Projectile damaged, measurement uncertain.
[b] Projectile did not perforate.
[c] Quantity could not be measured, projectile broke up.

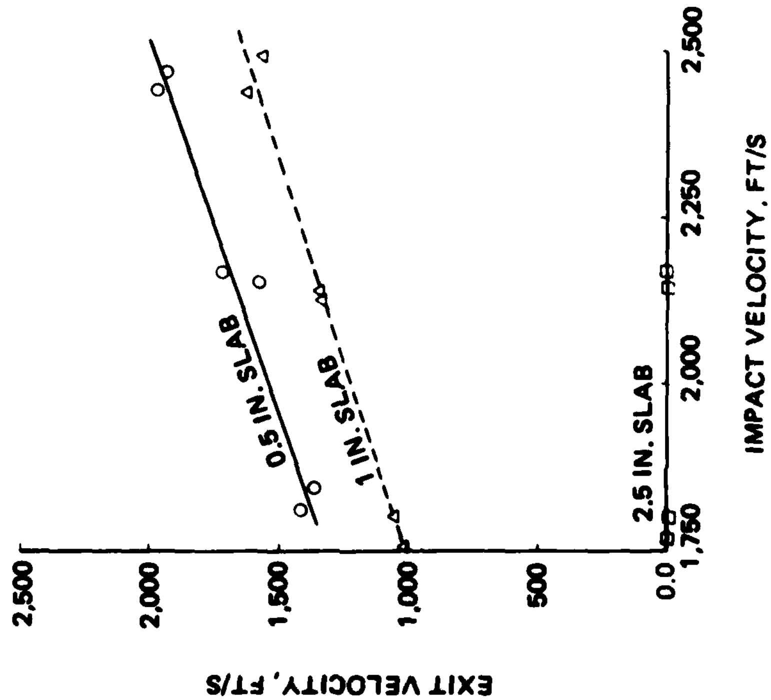

FIGURE 10. Exit Velocity vs. Impact Velocity for Unfilled Projectiles After Slab Impact at 45 Deg. Obliquity.

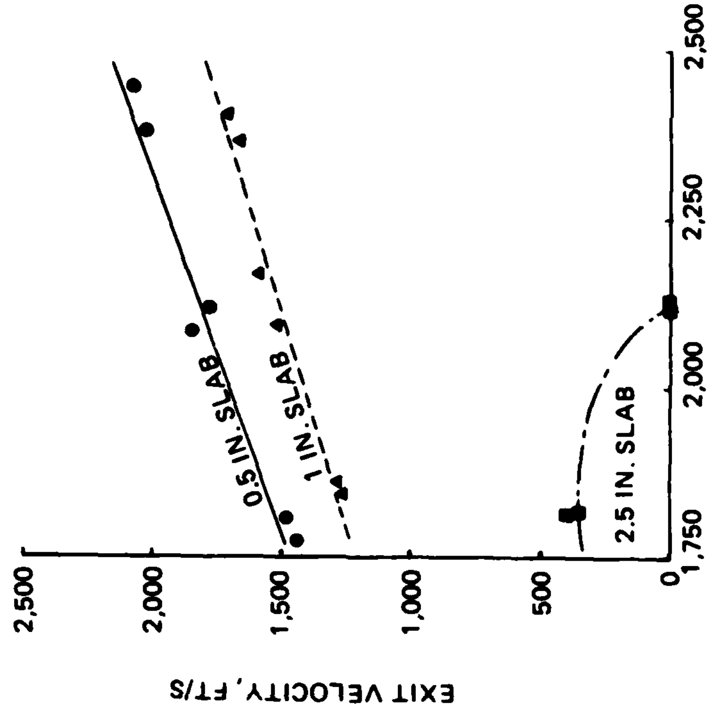

FIGURE 11. Exit Velocity vs. Impact Velocity for Filled Projectiles After Slab Impact at 45 Deg. Obliquity.

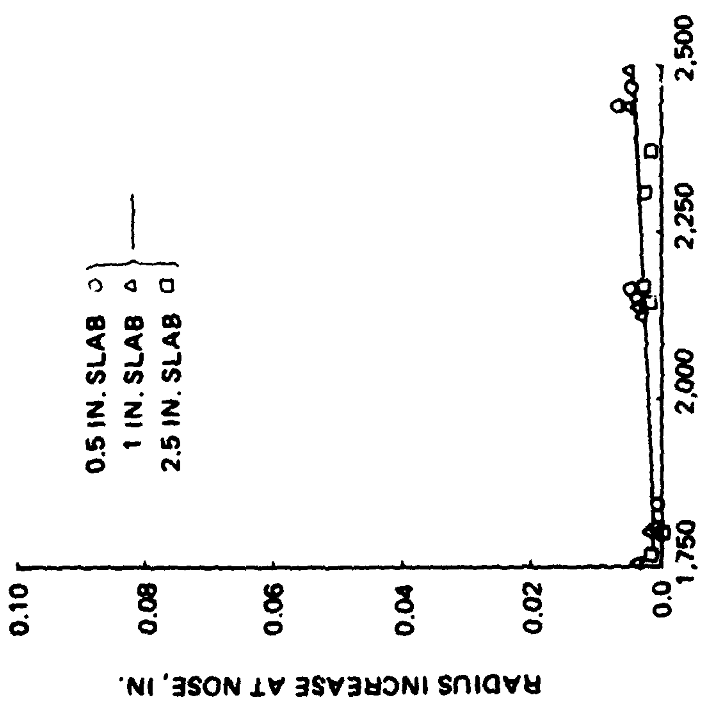

FIGURE 12. Radius Increase at Nose vs. Impact Velocity for Unfilled Projectiles After Slab Impact at 45 Deg. Obliquity.

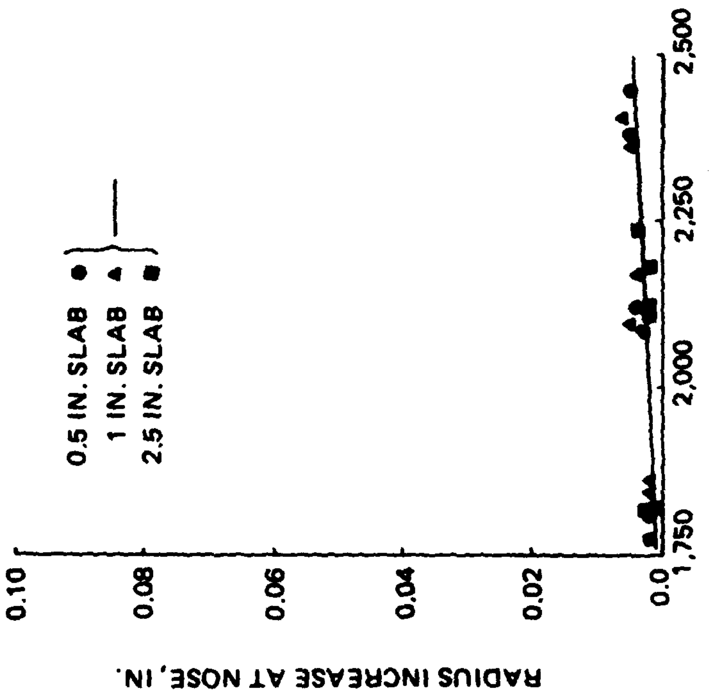

FIGURE 13. Radius Increase at Nose vs. Impact Velocity for Filled Projectiles After Slab Impact at 45 Deg. Obliquity.

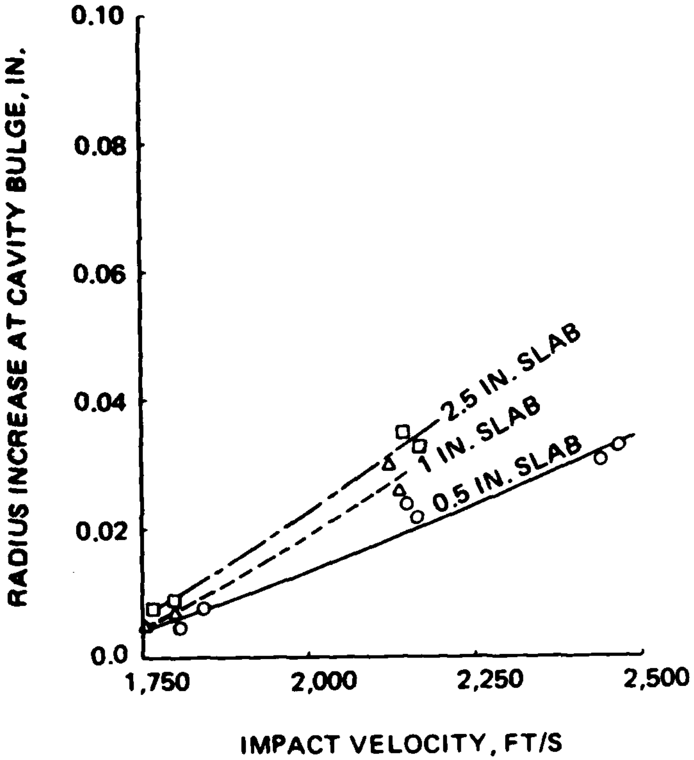

FIGURE 14. Radius Increase at Cavity Bulge vs. Impact Velocity for Unfilled Projectiles After Slab Impact at 45 Deg. Obliquity.

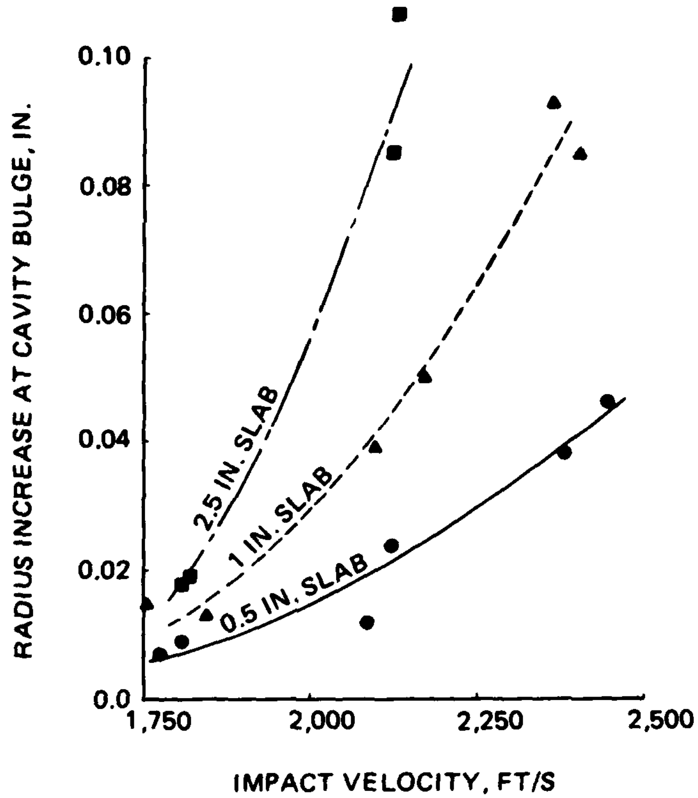

FIGURE 15. Radius Increase at Cavity Bulge vs. Impact Velocity for Filled Projectiles After Slab Impact at 45 Deg. Obliquity.

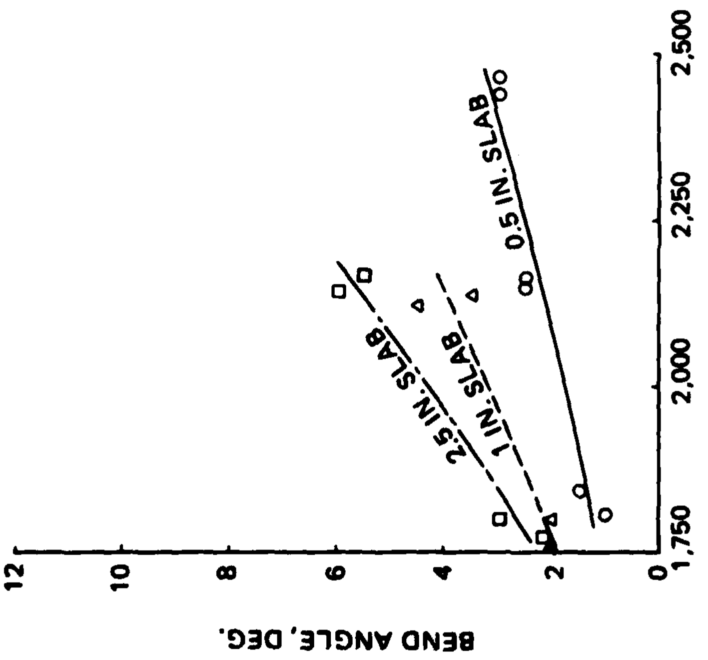

FIGURE 16. Bend Angle vs. Impact Velocity for Unfilled Projectiles After Slab Impact at 45 Deg. Obliquity.

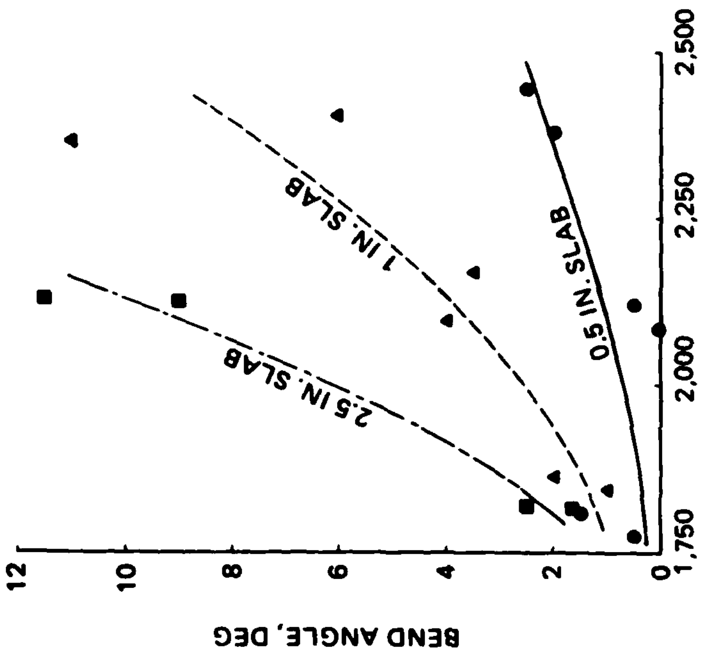

FIGURE 17. Bend Angle vs. Impact Velocity for Filled Projectiles After Slab Impact at 45 Deg. Obliquity.

shielded by a plug of target material. To shed some light on the possible formation of plugs on the projectiles used in the present experiments, an examination was made of the front surfaces of the test projectiles.

Photographs of the front surfaces of two projectiles (which can be taken as typical of all projectiles) are shown in Figure 18. Both projectiles were unfilled and were fired against 1-inch slabs at about 2,100 ft/s. One projectile impacted at normal incidence, the other at obliquity. After being photographed, the two projectiles were sectioned axially. The nose portions were then mounted, polished, etched, and subsequently studied using optical microscopy. The purpose of the microscopic examination was to help determine flow directions on the front surface.

The central region of the front surface of the projectile fired at normal incidence (Figure 18a) is heavily cratered, probably by impacts from sand grains in the Thorite. Much of the copper plating is still present. Except for localized areas around the craters, there is no evidence of flow of material in this region. Around the periphery of the front surface (outside of the central region) are a number of radial grooves. These are indicative of flow toward the outer edge, and microscopic examination confirmed that such flow did occur. The grooves were possibly formed by the abrasive action of the sand grains in the Thorite. The copper plating has been almost entirely removed from this portion.

The front surface of the projectile fired at obliquity (Figure 18b) shows a pattern of mostly unidirectional grooves fanning out slightly toward the bottom of the photograph (in the direction of the arrow). Again, the grooves were probably cut by the scouring action of the sand grains. Most of the copper plating has been removed from the front surface. Based on the photograph it would appear that flow was in the direction of the arrow. However, microscopic examination of the sectioned projectile indicated flow in the direction of the arrow over the lower two-thirds of the surface with some flow in the opposite direction in the upper third. The meaning of this opposite direction flow is not clear. Possibly it is a remnant of an earlier process. Radial grooves are visible near the lateral edge of the surface. It is likely that the radial grooves formed first because some of the unidirectional grooves appear to slice across them. Also present (but perhaps not visible on the reproduced photograph) are two roughly parallel grooves running at approximately right angles to the unidirectional grooves. These are believed to be imprints of the reinforcing wires striking the front surface.

With regard to plug formation on the front surface of projectiles in the current tests, the following speculations can be made.

1. The lack of flow on the central region of the front surface for projectiles fired at normal incidence is consistent with the presence of a stagnation zone which, in turn, is indicative of the presence of a plug. The radial flow near the periphery indicates that either this plug never covered the entire front surface or it did at one time and was subsequently eroded away.

2. The unidirectional nature of the flow across the front surface of projectiles fired at obliquity argues against the presence of a plug on this surface. However, it is possible that a plug could have formed early and been swept off the surface later. The radial grooves, which apparently formed before the unidirectional ones, are consistent with this possibility. Bending of the projectiles so that the front surface is no longer perpendicular to the direction

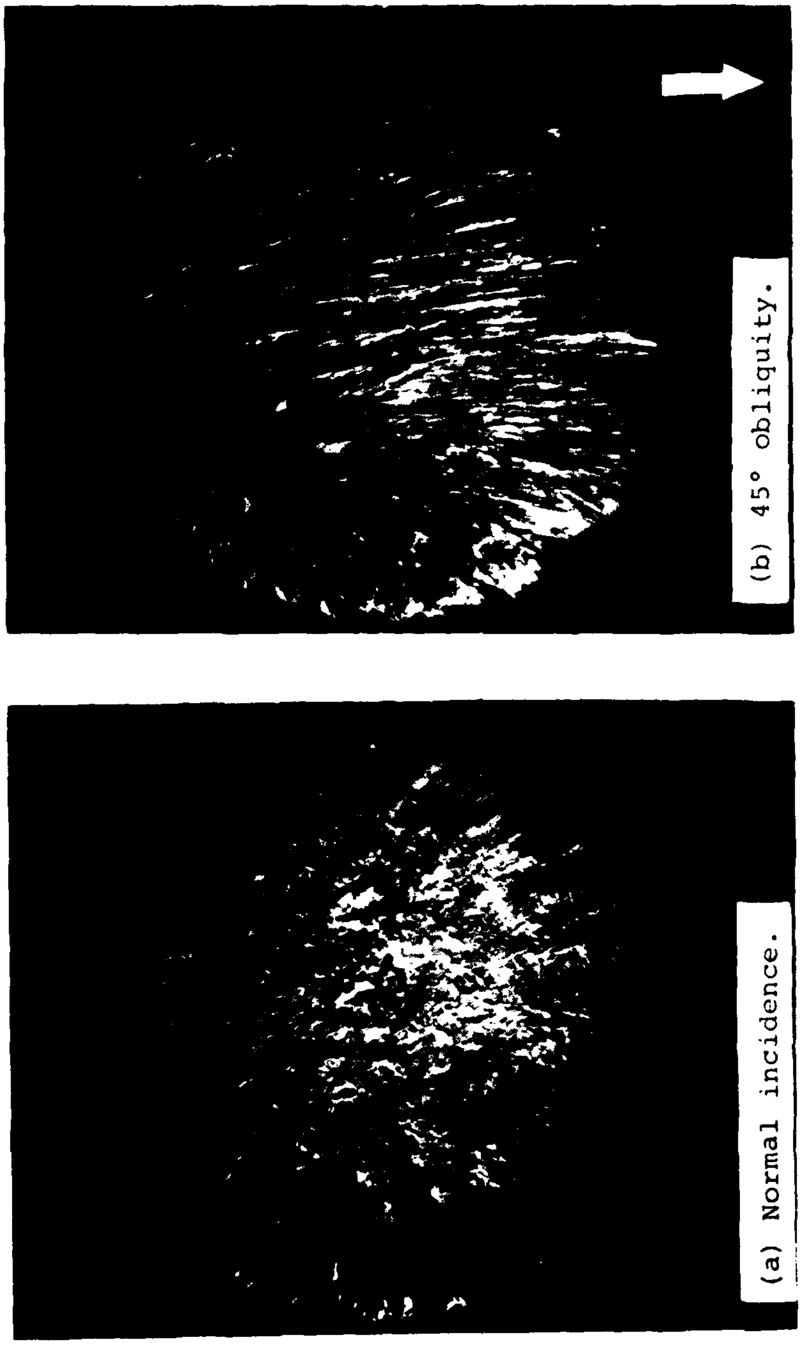

FIGURE 18. Photographs of Front Surface of Unfilled Projectiles After Impact at About 2,100 ft/s.

of motion may help initiate the transverse flow. The projectiles used in the report cited in footnote 6, on which plugs formed during oblique penetration of plaster of Paris, did not deform or bend.

CONCLUSION

The results of this experimental study provide a broad data base which can be used for verification of finite element structural analysis procedures. Some conclusions that can be drawn from the results of this study are

1. Mushrooming of the nose for the projectiles tested occurs very quickly and is associated with initial transients. The degree of mushrooming is significantly greater for normal incidence impacts where the target surface contacts the entire front surface of the projectile simultaneously.

2. Development of a bulge in the cavity region occurs more slowly. Bulge shape is strongly affected by the presence or absence of filler.

3. Bending in oblique impacts is strongly influenced by the presence or absence of filler.

4. It is likely that plugs of target material formed *on the front of the projectiles* fired at normal incidence. Projectiles fired at obliquity either never had plugs or these were wiped off at a later stage of the penetration process.

Appendix A
PHOTOGRAPHS OF PROJECTILES FIRED AT NORMAL INCIDENCE

(a) 1,795 ft/s

(b) 1,800 ft/s

(c) 2,110 ft/s

FIGURE A-1. Photographs of Unfilled Projectiles After Normal Incidence Impact Against 0.5-Inch-Thick Slabs.

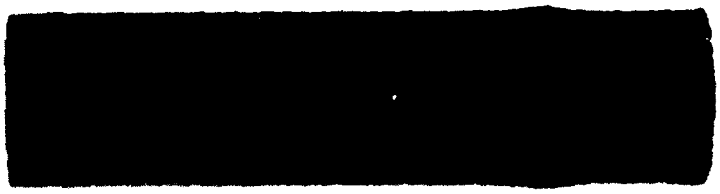

(d) 2,135 ft/s

(e) 2,370 ft/s

(f) 2,400 ft/s

FIGURE A-1. Contd.

(a) 1,785 ft/s

(b) 1,840 ft/s

(c) 2,110 ft/s

FIGURE A-2. Photographs of Unfilled Projectiles After Normal Incidence Impact Against 1-Inch-Thick Slabs.

(d) 2,160 ft/s

(e) 2,340 ft/s

(f) 2,405 ft/s

FIGURE A-2. Contd.

(a) 1,765 ft/s

(b) 1,800 ft/s

(c) 2,055 ft/s

FIGURE A-3. Photographs of Unfilled Projectiles After Normal Incidence Impact Against 2.5-Inch-Thick Slabs.

(d) 2,110 ft/s

(e) 2,365 ft/s

(f) 2,420 ft/s

FIGURE A-3. Contd.

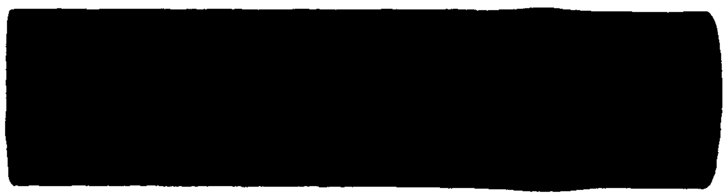

(a) 1,805 ft/s

(b) 1,810 ft/s

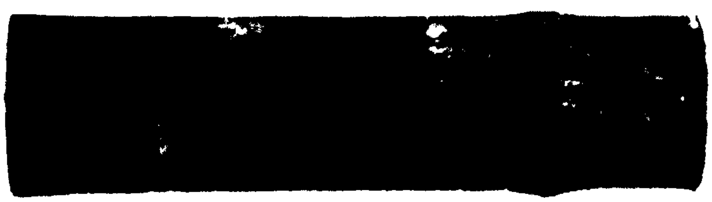

(c) 2,130 ft/s

FIGURE A-4. Photographs of Unfilled Projectiles After Normal Incidence Impact Against 5-Inch-Thick Slabs.

(d) 2,160 ft/s

(e) 2,410 ft/s

(f) 2,425 ft/s

FIGURE A-4. Contd.

(a) 1,770 ft/s

(b) 1,785 ft/s

(c) 2,070 ft/s

FIGURE A-5. Photographs of Filled Projectiles After Normal Incidence Impact Against 0.5-Inch-Thick Slabs.

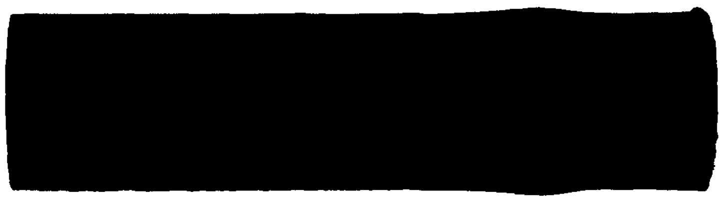

(d) 2,135 ft/s

(e) 2,380 ft/s

(f) 2,385 ft/s

FIGURE A-5. Contd.

(a) 1,825 ft/s

(b) 1,840 ft/s

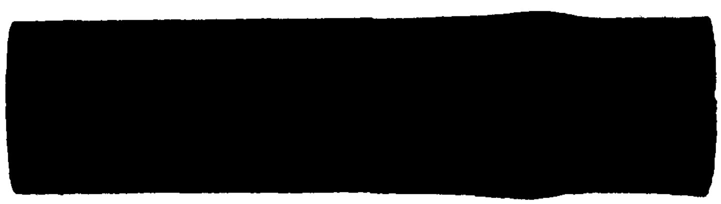

(c) 2,070 ft/s

FIGURE A-6. Photographs of Filled Projectiles After Normal Incidence Impact Against 1-Inch-Thick Slabs.

(d) 2,105 ft/s

(e) 2,370 ft/s

(f) 2,380 ft/s

FIGURE A-6. Contd.

(a) 1,755 ft/s

(b) 1,805 ft/s

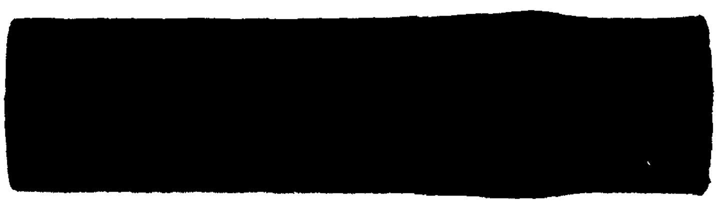

(c) 2,110 ft/s

FIGURE A-7. Photographs of Filled Projectiles After Normal Incidence Impact Against 2.5-Inch-Thick Slabs.

(d) 2,120 ft/s

(e) 2,360 ft/s

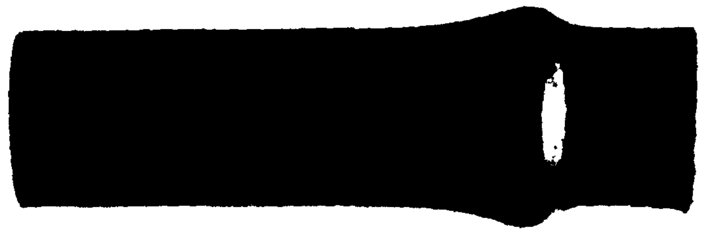

(f) 2,410 ft/s

FIGURE A-7. Contd.

(a) 1,770 ft/s

(b) 1,775 ft/s

(c) 2,045 ft/s

FIGURE A-8. Photographs of Filled Projectiles After Normal Incidence Impact Against 5-Inch-Thick Slabs.

(d) 2,130 ft/s

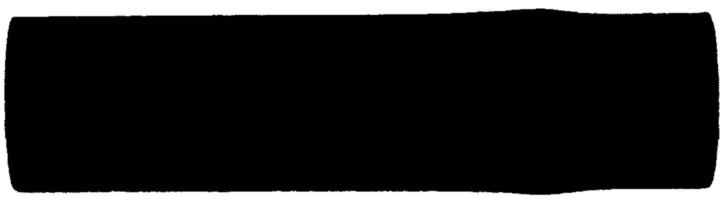

(e) 2,380 ft/s

(f) 2,400 ft/s

FIGURE A-8. Contd.

Appendix B
PHOTOGRAPHS OF PROJECTILES FIRED AT 45 DEGREES OBLIQUITY

(a) 1,807 ft/s

(b) 1,842 ft/s

(c) 2,150 ft/s

FIGURE B-1. Photographs of Unfilled Projectiles After Impact Against 0.5-Inch-Thick Slabs at 45 Degrees Obliquity.

(d) 2,165 ft/s

(e) 2,400 ft/s

(f) 2,440 ft/s

FIGURE B-1. Contd.

(a) 1,756 ft/s

(b) 1,800 ft/s

(c) 2,125 ft/s

FIGURE B-2. Photographs of Unfilled Projectiles After Impact Against 1-Inch-Thick Slabs at 45 Degrees Obliquity.

(d) 2,140 ft/s

(e) 2,440 ft/s

(f) 2,495 ft/s

FIGURE B-2. Contd.

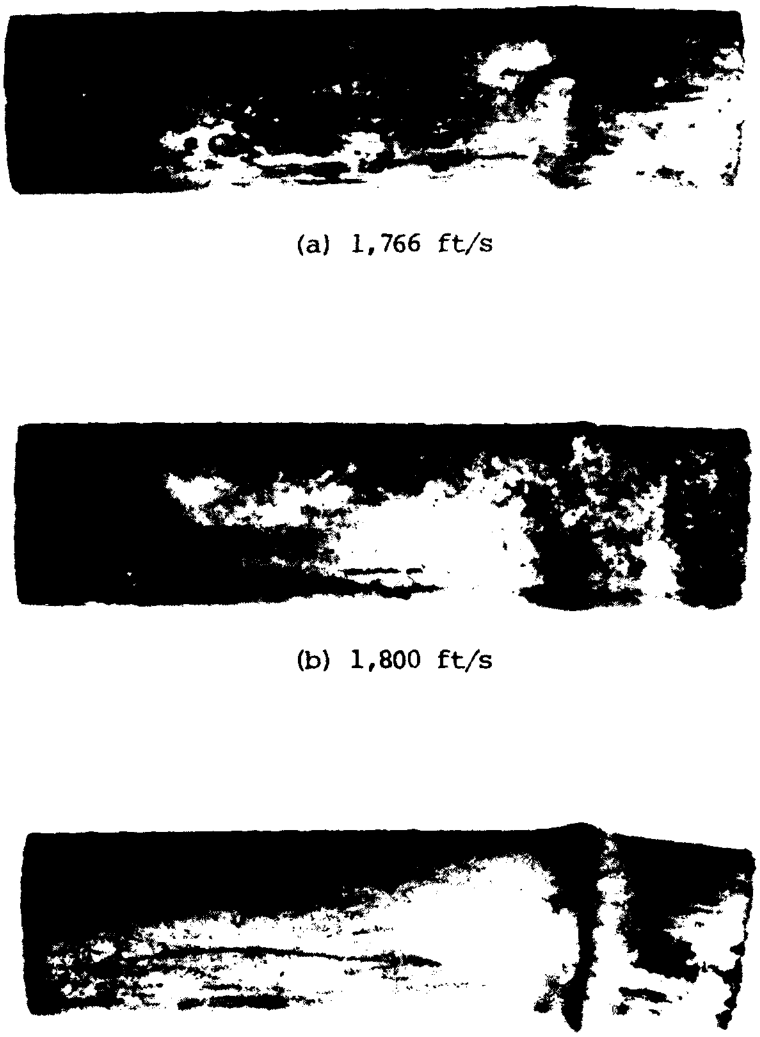

(a) 1,766 ft/s

(b) 1,800 ft/s

(c) 2,145 ft/s

FIGURE B-3. Photographs of Unfilled Projectiles After Impact Against 2.5-Inch-Thick Slabs at 45 Degrees Obliquity.

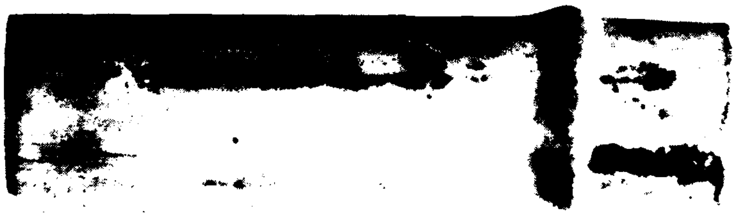

(d) 2,170 ft/s

(e) 2,310 ft/s

(f) 2,370 ft/s

FIGURE B-3. Contd.

(a) 1,773 ft/s

NOT PHOTOGRAPHED.

(b) 1,809 ft/s

(c) 2,085 ft/s

FIGURE B-4. Photographs of Unfilled Projectiles After Impact Against 0.5-Inch-Thick Slabs at 45 Degrees Obliquity.

(d) 2,120 ft/s

(e) 2,380 ft/s

(f) 2,445 ft/s

FIGURE B-4. Contd.

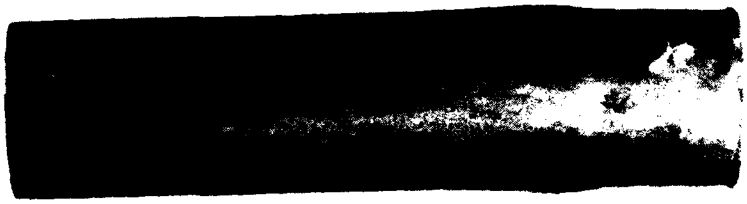

(a) 1,843 ft/s

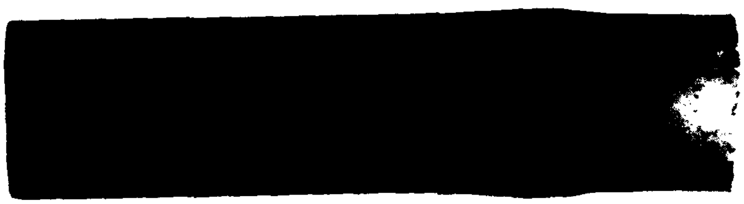

(b) 1,862 ft/s

(c) 2,095 ft/s

FIGURE B-5. Photographs of Filled Projectiles After Impact Against 1-Inch-Thick Slabs at 45 Degrees Obliquity.

(d) 2,170 ft/s

(e) 2,365 ft/s

(f) 2,405 ft/s

FIGURE B-5. Contd.

(a) 1,813 ft/s

(b) 1,815 ft/s

(c) 2,125 ft/s

FIGURE B-6. Photographs of Filled *Projectiles* After Impact Against 2.5-Inch-Thick Slabs at 45 Degrees Obliquity.

(d) 2,130 ft/s

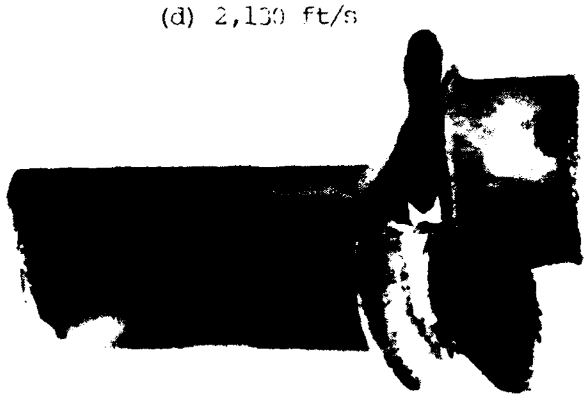

(e) 2,180 ft/s

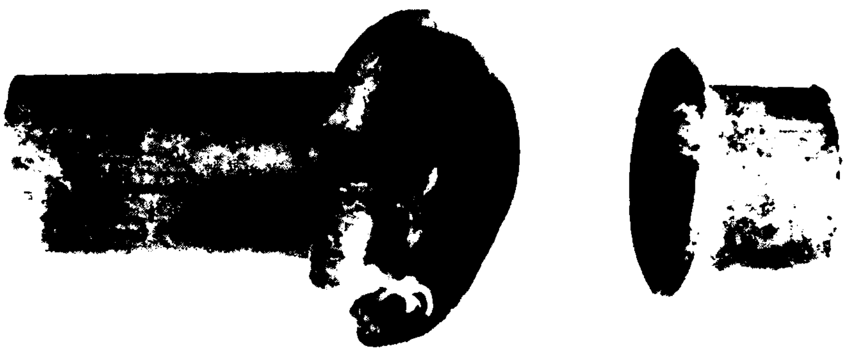

(f) 2,235 ft/s

FIGURE B-6. Contd.

INITIAL DISTRIBUTION

8 Naval Air Systems Command
  AIR-00D4 (2)
  AIR-301 (2)
  AIR-320 (1)
  AIR-320E (1)
  AIR-541 (2)
5 Chief of Naval Operations
  OP-03 (2)
  OP-05 (1)
  OP-098 (1)
  OP-55 (1)
2 Chief of Naval Material
  MAT-05 (1)
  MAT-08 (1)
1 Chief of Naval Research, Arlington (ONR-102)
7 Naval Sea Systems Command
  SEA-09B312 (2)
  SEA-62R (5)
1 Commander in Chief, U.S. Pacific Fleet (Code 325)
1 Commander, Third Fleet, Pearl Harbor
1 Commander, Seventh Fleet, San Francisco
1 Air Test and Evaluation Squadron 5
1 David W. Taylor Naval Ship Research and Development Center, Bethesda
1 Naval Air Force, Atlantic Fleet
2 Naval Air Force, Pacific Fleet
1 Naval Air Station, North Island
2 Naval Air Test Center, Patuxent River (CT-252, Bldg. 405 (Aeronautical Publications Library))
1 Naval Avionics Center, Indianapolis (Technical Library)
1 Naval Explosive Ordnance Disposal Technology Center, Indian Head
1 Naval Ocean Systems Center, San Diego (Code 131)
1 Naval Ordnance Station, Indian Head (Technical Library)
1 Naval Postgraduate School, Monterey
3 Naval Ship Weapon Systems Engineering Station, Port Hueneme
  Code 5711, Repository (2)
  Code 5712 (1)
5 Naval Surface Weapons Center, White Oak Laboratory, Silver Spring
  R-13, R. Liddiard (1)
  J. Erkman (1)
  S. Jacobs (1)
  Guided Missile Warhead Section (1)
  Technical Library (1)
1 Naval War College, Newport
1 Office of Naval Research, Pasadena Branch Office
1 Office of Naval Techology, Arlington (MAT-07)
1 Operational Test and Evaluation Force, Atlantic
1 Pacific Missile Test Center, Point Mugu (Technical Library)
1 Marine Air Base Squadron 32, Beaufort
1 Marine Corps Air Station, Beaufort

DATE
ILMED
8